Frascati Physics Series Vol. 66 (2018)
Frontier Objects in Astrophysics and Particle Physics
May 20-26, 2018

The Muon g-2 experiment at Fermilab: Run 1 Status and Perspectives

Marco Incagli*
INFN Pisa
on behalf of the Muon $g-2$ collaboration

Abstract

Since more than 50 years the electron and muon anomalies, a_e and a_μ, defined in terms of the gyromagnetic factor g_i for particle i as $a_i = (g_i - 2)/2$, have provided a deep insight into the quantum structure of elementary particles. They have been, and continue to be, a milestone for the development of the Standard Model of Particle Physics against which all new theories have to be compared. For almost 20 years, the experimental value of a_μ has shown a tantalizing discrepancy of more than 3σ from the theoretical prediction making it mandatory for experimentalists to improve the current result, dominated by the E821 experiment at BNL [1)].

The Muon $g-2$ E989 experiment at Fermilab will use the same storage ring technique used at BNL, and previously in the CERN-III experiment, with the goal of decreasing by a factor of 4 the current error on a_μ, which will allow for a finer comparison with the theoretical prediction. E989 started collecting data in winter 2018 accumulating, in the period April-July 2018 (Run1) almost twice the statistics of the previous experiment (before application of data quality cuts).

In this document, the experiment will be briefly described, underlying the improvements which will allow to reduce the systematic error, and some preliminary result will be shown.

1 Introduction

A particle with electric charge Q and spin $\vec{s}$ is characterized by a magnetic moment

$$\vec{\mu} = g\frac{Q}{2m}\vec{s} \tag{1}$$

where g is the gyromagnetic factor.

For an elementary spin 1/2 particle, Dirac theory predicts that the gyromagnetic ratio is exactly $g = 2$. However, the development of the Quantum ElectroDynamic theory (QED) led to the prediction, and then to the observation, of virtual diagrams in which photons, as well as other particles, are emitted and reabsorbed. These diagrams modify the effective magnetic momentum and therefore the coupling of the particle to an external magnetic field.

This was first predicted by Schwinger [2)] and measured by Kusch and Foley [3)] in 1948. At first level in perturbation theory, the anomaly a was predicted by Schwinger to be:

$$a = \frac{g-2}{2} = \frac{\alpha}{2\pi} = 0.00116 \pm 0.00004 \tag{2}$$

The mesaured value was:

$$a = 0.00118 \pm 0.00003 \tag{3}$$

It was the first great success of QED.

With time, the measurement has been refined over and over reaching the astonishing value of

$$a_e = (115965218073 \pm 28) \times 10^{-14}$$

for the electron [4)] and

$$a_\mu = (116592080 \pm 63) \times 10^{-11}$$

for the muon [1)].

Although the muon anomaly can be measured less precisely than the electron one, mostly beacause of the particle lifetime, it was soon realized that a new particle (boson) contributing to the anomaly in a virtual correction would have an effect which, in general, can be proportional to the square of the mass ratio:

$$\alpha_{NP} \simeq \left(\frac{m_\mu}{M}\right)^2$$

This is due to the chirality flip in the boson emission. Therefore the muon anomaly, although less precisely measured, is more sensitive to New Phisics contributions than the electron one.

The current precision with which the anomaly is known is summarized in table 1. The QED contribution has been evaluated at 5 loops (more than 12000 diagrams!), the electroweak contribution is well under control while the hadronic vacuum polarizion and the light-by-light scattering are the largest sources of uncertainty in the a_μ^{theo} determination.

Table 1: *Theoretical determination of muon anomaly* a_μ.

contribution	value ($\times 10^{-11}$)	error ($\times 10^{-11}$)	reference
QED	11658471.90	0.01	5)
EW	15.36	0.10	6)
LO HLbL	9.80	2.60	7)
NLO HLbL	0.30	0.20	8)
LO HVP	693.27	2.46	9)
NLO HVP	-9,82	0.04	9)
NNLO HVP	1.24	0.01	10)
Total	11659182.05	3.56	9)

The theoretical prediction shows a tantalizing discrepancy of 3.7σ from the experimental result quoted above, which calls for a new experiment to possibly confirm, with a larger significance, the current difference.

The Muon $g-2$ experiment at Fermilab is designed to measure the muon anomaly with an error 4 times smaller than the current one by using the same experimental technique used in BNL as well as in the CERNIII experiment, briefly described in the next section, but improving both on the statistical and on the systematical error. In particular, the E821 total error was dominated by

the statistical component, therefore the first goal of the Fermilab experiment is to increase the collected statistics by a factor of 21, while the systematical error will have to be improved "just" by a factor of 3 to reach the final sensitivity.

2 The experiment

The experiment is based on the principle that the spin of a muon moving in a constant magnetic field $\vec{B}$, in the presence of a static electric field $\vec{E}$, precesses around $\vec{B}$ with an angular velocity ω_s which is slightly faster than the momentum precession (cyclotron frequency) ω_p around the same vector. More precisely, the spin vector projection on the momentum axis changes with time according to (from [12] eq.11.171):

$$\frac{d}{dt}(\hat{\beta}\cdot\vec{s}) = -\frac{e}{mc}\vec{s}_{\perp}\cdot\left[\left(\frac{g}{2}-1\right)\hat{\beta}\times\vec{B}+\left(\frac{g\beta}{2}-\frac{1}{\beta}\right)\vec{E}\right] \tag{4}$$

For a muon beam of momentum $p_\mu = 3.095$ GeV/c, called *magic momentum*, corresponding to a value of β which cancels out the second term of equation 4, and assuming that all muons follow the ideal circular path in a plane perpendicular to $\vec{B}$, then the above expression greatly simplifies into:

$$\omega_a = \frac{ea_\mu B}{m} \tag{5}$$

where $\omega_a = \omega_s - \omega_p$ is the difference between the spin precession and the cyclotron frequency and where quantities are taken as absolute values (no sign). By inverting the simplified equation 5, the the muon anomaly a_μ is given by:

$$a_\mu = \frac{m\omega_a}{eB} \tag{6}$$

In reality, the beam will have dimensions both in the radial and in the vertical directions, as well as a momentum spread, therefore the simple expression given above is only a first order approximation which will need to be carefully corrected. The most evident correction to the motion is the so-called *Coherent Betatron Oscillation* (CBO), which is due to the radial and vertical movement of particles within the beam. This will be briefly discussed in section 4.

3 The E989 experiment at Fermilab

The E989 experiment at Fermilab is largely built on the legacy of E821. During the summer of 2013, the 14-m diameter superconducting coils from the E821

storage magnet were moved from Brookhaven National Laboratory in New York to Fermilab, near Chicago. Performing the experiment at Fermilab provides a number of advantages, including the ability to produce more muons and to eliminate the pion contamination of the muon beam injected into the storage ring, which was a major limiting factor for E821.

The upgraded linear accelerator and booster ring structure of FNAL will deliver proton pulses (8 GeV, 4×10^{12} protons per pulse, 1.3 s pulse separation) impinging on the production target. The secondary π^+ beam will be focused with a pulsed lithium lens into the transport beam line which accepts π^+ with a momentum spread of $\pm 0.5\%$ around 3.11 GeV/c. In the transport beam line and in the delivery ring section the in-flight-decay of π^+ generates the μ^+ beam, polarized due to the V-A structure of the weak current. The $\simeq 10$ times longer flight distance at FNAL compared to BNL allows the residual hadronic contamination in the muon beam to decay away before it reaches the muon storage ring. This will essentially eliminate the so called hadronic flash in the positron calorimeters after muon beam injection which was a major source of background for the BNL experiment. The muons are injected into the storage ring through an inflector magnet which locally cancels out the main dipole field, thus allowing the muons to enter the storage ring perpendicularly to its radius at a value which is 77 mm larger than the nominal one. A set of kickers then kicks the muons into the right orbit. Muons then circulate in the storage ring decaying with a lifetime $\tau = \gamma\tau_0 \simeq 64\,\mu$s. The high-energy positrons from the muon decay are emitted preferentially along the spin direction, again because of the V-A structure of the weak current, with an asymmetry A which depends on the positron fractional energy.

Twenty-four individual calorimeter stations [11], each consisting of an array of 6×9 PbF2 crystals (25.4 mm $\times$ 25.4 mm $\times$ 152.4 mm) will be spaced equidistantly around the inner radius of the storage ring in order to capture the emitted positrons. Each crystal is individually instrumented with a silicon photomultiplier (SiPM) to detect the Cerenkov light generated by the high energy positrons. The high segmentation allows hit position discrimination while the fast SiPM response can separate events as close as 3 ns (800 MHz digitization rate) which will allow to address pile-up related systematic effects.

A sophisticated laser system will be used to calibrate in energy and to align in time the response of the 1296 crystals. This is of paramount importance

as the single largest systematic error in the BNL experiment was the calorimeter "gain stability", corresponding to 120 ppb error contribution out of a total of $\sigma_{\omega A}^{syst} = 180$ ppb [1]. Thanks to the laser system and to the new calorimeter, the budget for this error is 20 ppb: a reduction of a factor 6!

Straw tracker stations will be operated in front of two positron calorimeters which will allow for the precise reconstruction of the positron flight path and of the muon beam distribution. Retractable fiber harp detectors will be installed in the muon storage region to measure the muon distribution in the storage region.

4 Current status

E989 started collecting data in February 2018. After few months of commissioning, the first real data started to accumulate in April of the same year which allowed to reach by the end of Run1 in July 2018, a raw integral number of positrons which is almost twice the total sample of the previous BNL experiment.

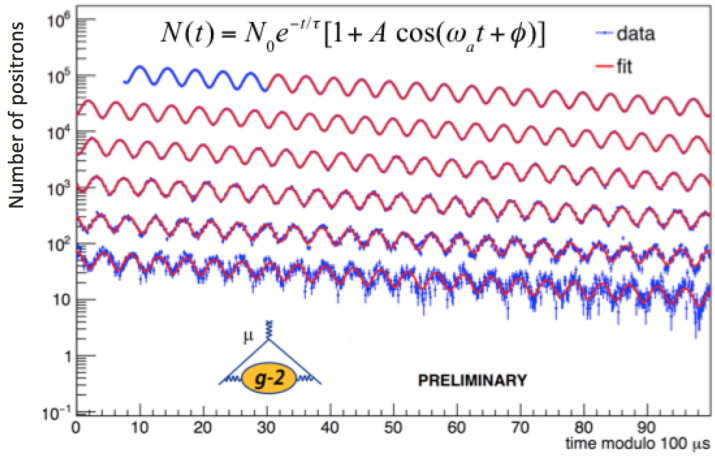

Figure 1: Arrival time spectrum of high energy positrons from a subset of data. The data are fit with an exponentional decay modulated by a sinusoidal function describing the muon spin precession.

Although Data Quality Cuts have still to be applied, with some simple cuts it is possible to produce the plot of fig.1 obtained by selecting positrons events with an energy larger than 1.7 GeV in a sample corresponding to one day of data taking acquired at the beginnig of April 2018. The plot shows the spin precession with respect to the cyclotron frequency modulating the muon exponential decay. The modulation is characterized by an amplitude A which depends on the specific energy cut applied to data.

The higher the energy cut, the higher the asymmetry parameter A. At the same time, however, by increasing the energy threshold the number of observed positrons N decreases, thus reducing the statistical significance. The optimal value is obtained by maximizing the product A^2N, which corresponds to a threshold $E_{thr} = 1.7$ GeV.

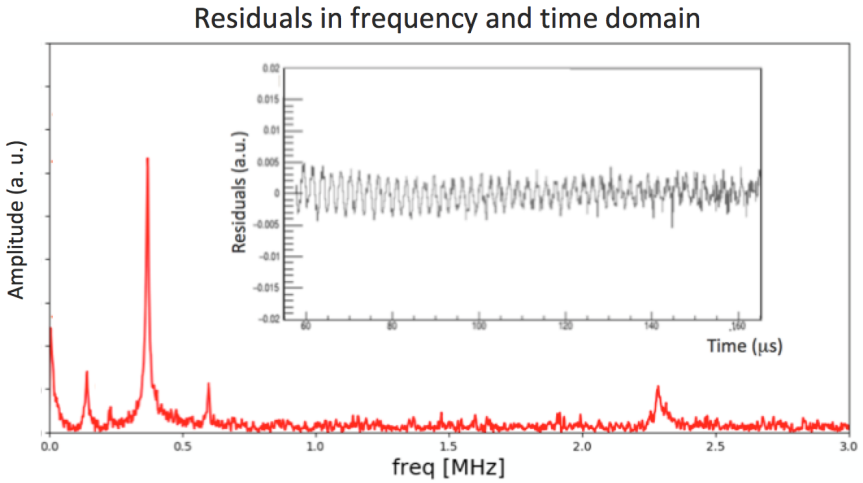

Figure 2: Residuals between function and data in the preliminary fit shown in the previous figure in the frequency and in the time domain. It is evident a residual fluctuation mostly due to Coherent Betatron Oscillations. Other minor peaks are visibles due to additional beam effects (see text).

The fit shows a very good qualitative agreement with data, given the statistics. However in fig.2 the residuals (data–fit) are plotted, both in the time and in the frequency domain. It is evident an oscillation which peaks at

$\simeq$ 370 kHz. This is due to beam Coherent Betatron Oscillations. The CBO modulation is physically caused by a mismatch between the emittance of the inflector and the acceptance of the storage ring. It causes the beam to oscillate radially with a frequency, as seen by a fixed detector, close to twice the $g-2$ one. It must be included in the fit, by adding extra-parameters, but it will also be studied independently with the tracking system, able to follow the beam profile, and the muon directions, in different locations around the ring.

5 Conclusion

The Muon $g-2$ experiment E989 at Fermilab started to collect data with the aim of improving by a factor 4 the precision of the previous BNL experiment.

A statistics larger than the one integratd at BNL has already been collected in Run 1 (April-July 2018).

The present muon storage rate is below that projected in the TDR by almost a factor of 2; several improvements are foreseen to be installed in Summer 2018, both in the accelerator complex and in the storage ring, which will allow to recover the design rate. In particular the interface between the two systems, the inflector, will be replaced with a new one, currently under test, which will be installed before the start of Run 2 (Oct, 1st 2018).

A preliminary analysis of the first collected data shows that the new systems installed in E989 (new segmented calorimeter, laser calibration system, straw tracker,...) are working as expected and they seem to be able to keep the systematic error at or below their budget.

If the E989 will confirm the previously measured value, then this could provide a 7σ discrepancy from the Standard Model, which would be a strong indication for new, as yet undiscovered, particles in loops which contribute to the muon anomaly.

6 Acknowledgments

This work was supported by Istituto Nazionale di Fisica Nucleare, the US DOE, Fermilab, and the EU Horizon 2020 Research and Innovation Program under the Marie Sklodowska-Curie Grant Agreement No.690385 and No.734303.

References

1. H. N. Brown et al. [Muon g-2 Collaboration], Phys. Rev. Lett. 86 (2001) 2227
2. J. Schwinger, Phys. Rev. 74 (1948) 416
3. P. Kusch, H. M. Foley, Phys. Rev. 74 (1948) 421
4. D. Hanneke *et al*, Phys. Rev. A. 83 (5): 052122
5. T. Aoyama *et al*, arXiv:1712:06060
6. C. Gnendiger *et al*, Phys. Rev. D88 (2013) 053005
7. F Jegerlehner, EPJ Web Conf 118 (2016) 01016
8. G. Colangelo *et al*, Phys. Lett. B735 (2014) 90
9. A. Keshavarzi *et al*, Phys. Rev. D 97, 114025
10. A. Kurz *et al*, Phys. Lett. B 734 (2014) 144
11. J. Kaspar, *et al*, JINST 12 (2017) no.01, P01009
12. J. D. Jackson, "Classical electrodynamics"